JOC Article

Design, Synthesis, and Biological Evaluation of Novel C14−C3′BzN-Linked Macrocyclic Taxoids†

Liang Sun,‡ Xudong Geng,‡ Raphaël Geney,‡ Yuan Li,‡ Carlos Simmerling,‡,§ Zhong Li,‡ Joseph W. Lauher,‡ Shujun Xia,|| Susan B. Horwitz,|| Jean M. Veith,⊥ Paula Pera,⊥ Ralph J. Bernacki,⊥ and Iwao Ojima*,‡,§

Department of Chemistry, State University of New York at Stony Brook, Stony Brook, New York 11794−3400, Institute of Chemical Biology & Drug Discovery, State University of New York at Stony Brook, Stony Brook, New York 11794-3400, Department of Molecular Pharmacology, Albert Einstein College of Medicine, Bronx, New York 10461, and Department of Pharmacology and Therapeutics, Roswell Park Cancer Institute, Elm and Carlton Streets, Buffalo, New York 14263

iojima@notes.cc.sunysb.edu

Received August 1, 2008

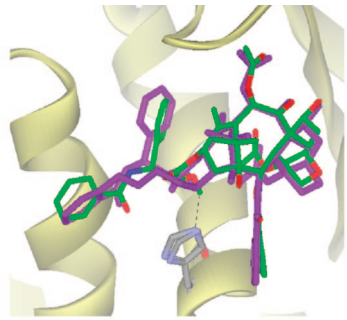

Novel macrocyclic taxoid closely mimicking the potency and bioactive conformation of paclitaxel

Novel macrocyclic paclitaxel congeners were designed to mimic the bioactive conformation of paclitaxel. Computational analysis of the "REDOR-Taxol" structure revealed that this structure could be rigidified by connecting the C14 position of the baccatin moiety and the *ortho* position of C3′*N*-benzoyl group (C3′BzN), which are ca. 7.5 Å apart, with a short linker (4−6 atoms). 7-TES-14β-allyloxybaccatin III and (3*R*,4*S*)-1-(2-alkenylbenzoyl)-β-lactams were selected as key components, and the Ojima−Holton coupling afforded the corresponding paclitaxel-dienes. The Ru-catalyzed ring-closing metathesis (RCM) of paclitaxel-dienes gave the designed 15- and 16-membered macrocyclic taxoids. However, the RCM reaction to form the designed 14-membered macrocyclic taxoid did not proceed as planned. Instead, the attempted RCM reaction led to the occurrence of an unprecedented novel Ru-catalyzed diene-coupling process, giving the corresponding 15-membered macrocyclic taxoid (SB-T-2054). The biological activities of the novel macrocyclic taxoids were evaluated by tumor cell growth inhibition (i.e., cytotoxicity) and tubulin-polymerization assays. Those assays revealed high sensitivity of cytotoxicity to subtle conformational changes. Among the novel macrocyclic taxoids evaluated, SB-T-2054 is the most active compound, which possesses virtually the same potency as that of paclitaxel. The result may also indicate that SB-T-2054 structure is an excellent mimic of the bioactive conformation of paclitaxel. Computational analysis for the observed structure−activity relationships is also performed and discussed.

Introduction

Cancer has become the leading cause of death for people under the age of 85 in the US.[1,2] Paclitaxel is currently one of the most widely used drugs in the fight against cancer among a variety of chemotherapeutic agents.[3,4] Paclitaxel binds to the β-tubulin subunit, accelerates the polymerization of tubulin, and stabilizes the resultant microtubules, which leads to apoptosis through cell-signaling cascade.[5,6] Investigation into the bioactive conformation of paclitaxel[7,8] would lead to the development of novel drugs with much simpler structures and the same or even higher activity.

The polar and nonpolar conformations of paclitaxel were first proposed on the basis of the structural analysis in solution and in the solid state using NMR and X-ray crystallography.[9−13]

* To whom correspondence should be addressed: Phone: 631-632-1339. Fax: 631-632-7942.

† This paper is dedicated to late Professor Albert I. Meyers for his life-long outstanding contributions to the advancement of synthetic organic chemistry, his exceptional leadership and mentorship in the field, as well as for numerous fond memories of him and his warm and caring personality with big heart.

‡ Department of Chemistry, State University of New York at Stony Brook.
§ Institute of Chemical Biology & Drug Discovery.
|| Albert Einstein College of Medicine.
⊥ Roswell Park Cancer Institute.

10.1021/jo801713q CCC: $40.75
Published on Web 11/01/2008

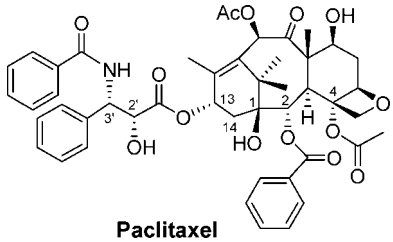

Paclitaxel

Organic and medicinal chemists designed a series of structurally restrained taxoids to mimic these two conformations, but all of the synthesized taxoids were substantially less active than paclitaxel.[7,14−16] The structural biology study of paclitaxel did not start until the first cryo-electron microscopy (cryo-EM) structure of paclitaxel-bound Zn^{2+}-stabilized α,β-tubulin dimer was reported in 1998 at 3.7 Å resolution (1TUB structure),[17] which used the docetaxel crystal structure for display. The 1TUB structure was later refined to 3.5 Å resolution with a paclitaxel molecule (1JFF structure) in 2001.[18] However, the resolution of these cryo-EM structures was not high enough to solve the binding conformation of paclitaxel. Thus, a computational study of the electron-density map was performed, which led to the proposal of the "T-Taxol" conformation.[19] To prove the validity of the "T-Taxol" structure, rigidified paclitaxel congeners were designed, synthesized, and assayed for their tubulin polymerization ability and cytotoxicity.[7,20−23] Among those "T-Taxol" mimcs, C4−C3′-linked macrocyclic taxoids showed higher activities than paclitaxel in the cytotoxicity and tubulin-polymerization assays.[20,22]

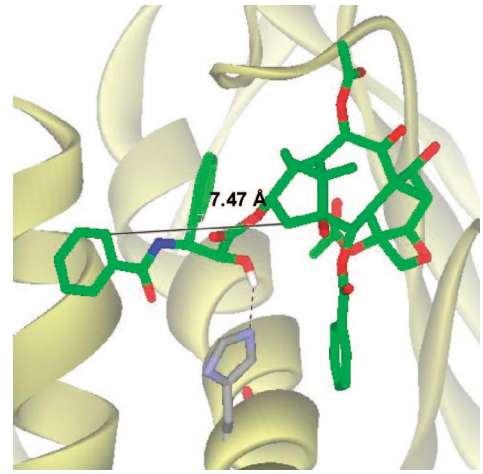

FIGURE 1. REDOR-Taxol-1JFF and the atom−atom distance between C14 and the *ortho* carbon of the C3′N-benzoyl group.

In the meantime, two $^{13}C-^{19}F$ intramolecular distances of the microtubule-bound 2-(4-fluorobenzoyl)paclitaxel were experimentally obtained by means of the REDOR NMR study in 2000.[24] On the basis of the REDOR distances, MD analysis of paclitaxel conformers, photoaffinity labeling,[25] and molecular modeling studies using the 1TUB coordinate,[17] we proposed the "REDOR-Taxol" as a valid microtubule-bound paclitaxel structure in 2005.[8] We have further refined the "REDOR-Taxol" using the 1JFF coordinate and found that the "REDOR-Taxol" is not only fully consistent with the new REDOR-experiments[26] but also accommodates highly active macrocyclic paclitaxel analogues designed on the basis of the "T-Taxol" structure (see the Supporting Information). The critical difference between these two structures is the orientation of the C2′-OH group. In the "REDOR-Taxol", the C2′-OH group interacts with His^{227} as the hydrogen bond donor,[8] while the H-bonding is between the C2′-OH and the backbone carbonyl oxygen of Arg^{369} in the "T-Taxol".[19] Accordingly, we have designed novel macrocyclic taxoids by linking the C14 and C3′BzN groups, which mimic the "REDOR-Taxol" structure to examine whether these conformationally restricted taxoids exhibit the same level of biological activity as that of paclitaxel.

Results and Discussion

Design of Novel C14−C3′BzN-Linked Macrocyclic Taxoids. Computational analysis of the "REDOR-Taxol" revealed that this structure could be rigidified by connecting the C14 position of the baccatin moiety and the *ortho* position of C3′*N*-benzoyl group (C3′BzN), which are ca. 7.5 Å apart, with a short linker (4−6 atoms) (Figure 1). Also, the same analysis indicated that the use of such linkers would not interfere with the amino acid residues in the paclitaxel binding site. Since the naturally occurring 14β-OH-10-deacetylbaccatin (14-OH-DAB) is readily available to us and we have performed substantial SAR studies on the taxoids derived from this material, we chose 14-OH-

(1) Jemal, A.; Ward, E.; Hao, Y.; Thun, M. *JAMA, J. Am. Med. Assoc.* **2005**, *294*, 1255–1259.
(2) Jemal, A.; Siegel, R.; Ward, E.; Murray, T.; Xu, J.; Smigal, C.; Thun Michael, J. *Ca−Cancer J. Clin.* **2006**, *56*, 106–130.
(3) Rowinsky, E. K. *Ann. Rev. Med.* **1997**, *48*, 353–374.
(4) Suffness, M., Ed. *Taxol: Science and Applications*, **1995**.
(5) Schiff, P. B.; Fant, J.; Horwitz, S. B. *Nature* **1979**, *277*, 665–667.
(6) Schiff, P. B.; Horwitz, S. B. *Proc. Natl. Acad. Sci. U.S.A.* **1980**, *77*, 1561–1565.
(7) Kingston, D. G. I.; Bane, S.; Snyder, J. P. *Cell Cycle* **2005**, *4*, 279–289.
(8) Geney, R.; Sun, L.; Pera, P.; Bernacki, R. J.; Xia, S.; Horwitz, S. B.; Simmerling, C. L.; Ojima, I. *Chem. Biol.* **2005**, *12*, 339–348.
(9) Dubois, J.; Guenard, D.; Gueritte-Voegelein, F.; Guedira, N.; Potier, P.; Gillet, B.; Beloeil, J. C. *Tetrahedron* **1993**, *49*, 6533–6544.
(10) Williams, H. J.; Scott, A. I.; Dieden, R. A.; Swindell, C. S.; Chirlian, L. E.; Francl, M. M.; Heerding, J. M.; Krauss, N. E. *Tetrahedron* **1993**, *49*, 6545–6560.
(11) Vander Velde, D. G.; Georg, G. I.; Grunewald, G. L.; Gunn, C. W.; Mitscher, L. A. *J. Am. Chem. Soc.* **1993**, *115*, 11650–11651.
(12) Mastropaolo, D.; Camerman, A.; Luo, Y.; Brayer, G. D.; Camerman, N. *Proc. Natl. Acad. Sci. U.S.A.* **1995**, *92*, 6920–6924.
(13) Ojima, I.; Kuduk, S. D.; Chakravarty, S.; Ourevitch, M.; Bégué, J.-P. *J. Am. Chem. Soc.* **1997**, *119*, 5519–5527.
(14) Ojima, I.; Lin, S.; Inoue, T.; Miller, M. L.; Borella, C. P.; Geng, X.; Walsh, J. J. *J. Am. Chem. Soc.* **2000**, *122*, 5343–5353.
(15) Ojima, I.; Zucco, M.; Duclos, O.; Kuduk, S. D.; Sun, C.-M.; Park, Y. H. *Bioorg. Med. Chem. Lett.* **1993**, *3*, 2479–2482.
(16) Geng, X.; Miller, M. L.; Lin, S.; Ojima, I. *Org. Lett.* **2003**, *5*, 3733–3736.
(17) Nogales, E.; Wolf, S. G.; Downing, K. H. *Nature* **1998**, *391*, 199–203.
(18) Lowe, J.; Li, H.; Downing, K. H.; Nogales, E. *J. Mol. Bol.* **2001**, *313*, 1045–1057.
(19) Snyder, J. P.; Nettles, J. H.; Cornett, B.; Downing, K. H.; Nogales, E. *Proc. Natl. Acad. Sci. U.S.A.* **2001**, *98*, 5312–5316.
(20) Ganesh, T.; Guza, R. C.; Bane, S.; Ravindra, R.; Shanker, N.; Lakdawala, A. S.; Snyder, J. P.; Kingston, D. G. I. *Proc. Natl. Acad. Sci. U.S.A.* **2004**, *101*, 10006–10011.
(21) Querolle, O. D., J.; Thoret, S.; Roussi, F.; Gueritte, F.; Guénard, D. *J. Med. Chem.* **2004**, *47*, 5937–5944.
(22) Ganesh, T.; Yang, C.; Norris, A.; Glass, T.; Bane, S.; Ravindra, R.; Banerjee, A.; Metaferia, B.; Thomas, S. L.; Giannakakou, P.; Alcaraz, A. A.; Lakdawala, A. S.; Snyder, J. P.; Kingston, D. G. I. *J. Med. Chem.* **2007**, *50*, 713–725.
(23) Larroque, A.-L.; Dubois, J.; Thoret, S.; Aubert, G.; Chiaroni, A.; Gueritte, F.; Guenard, D. *Bioorg. Med. Chem.* **2007**, *15*, 563–574.
(24) Li, Y.; Poliks, B.; Cegelski, L.; Poliks, M.; Cryczynski, A.; Piszcek, G.; Jagtap, P. G.; Studelska, D. R.; Kingston, D. G. I.; Schaefer, J.; Bane, S. *Biochemistry* **2000**, *39*, 281–291.
(25) Rao, S.; He, L.; Chakravarty, S.; Ojima, I.; Orr, G. A.; Horwitz, S. B. *J. Biol. Chem.* **1999**, *274*, 37990–37994.
(26) Paik, Y.; Yang, C.; Metaferia, B.; Tang, S.; Bane, S.; Ravindra, R.; Shanker, N.; Alcaraz, A. A.; Johnson, S. A.; Schaefer, J.; O'Connor, R. D.; Cegelski, L.; Snyder, J. P.; Kingston, D. G. I. *J. Am. Chem. Soc.* **2007**, *129*, 361–370.

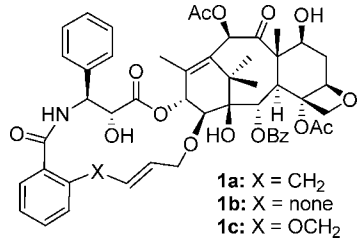

FIGURE 2. Designed novel C14−C3′BzN-linked macrocyclic taxoids.

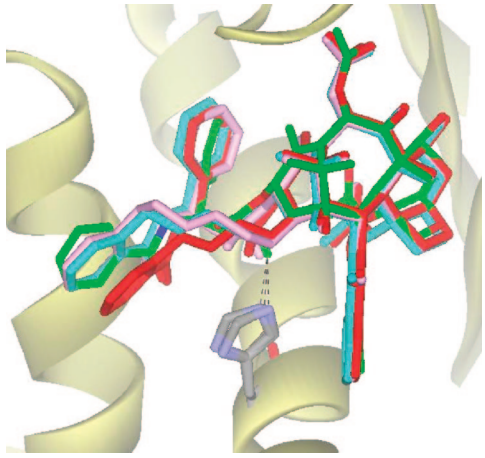

FIGURE 3. Overlays of REDOR-Taxol (green) with **1a** (cyan), **1b** (red), and **1c** (pink).

DAB as a key starting material for the synthesis of novel macrocyclic taxoids. Thus, the C14 position of the designed novel taxoids was fixed to β-ether functionality. The structures of the designed macrocyclic taxoids are shown in Figure 2. As the overlays in Figure 3 illustrate, the designed macrocyclic taxoids **1a** and **1c** appear to mimic the REDOR-Taxol structure very well, while the C3′*N*-benzoyl group of **1b** deviates from the rest.

In addition, we included a C3′-(2-methylpropen-2-yl) analogue of **1a**, i.e., **1d**, for comparison, since the replacement of the 3′-phenyl moiety with a 3′-(2-methylpropen-2-yl) group in paclitaxel and docetaxel produced the corresponding taxoids with higher potency.[27,28]

Synthesis of Macrocyclic Taxoids. As the retrosynthetic analysis in Scheme 1 shows, the designed C14−C3′BzN-linked macrocyclic taxoids **1a**−**c** can be synthesized through ring-closing metathesis (RCM)[29] of diene key intermediates **7a**−**c**, which can be obtained from the corresponding (3*R*,4*S*)-1-(2-alkenylbenzoyl)-β-lactam **3a**−**c** and 14β-allyloxybaccatin **6** through the Ojima−Holton coupling.[14,15,27,30,31] A similar strategy worked very well previously for the synthesis of the C2−C3′-linked[14,32] and C2−C3′*N*-linked[33] macrocyclic taxoids in our laboratory. Macrocyclic taxoid **1d** can be synthesized just by using (3*R*,4*S*)-4-(2-methylpropen-2-yl)-β-lactam **3d** in place of **3a**−**c**.

As Scheme 2 shows, (3*R*,4*S*)-β-lactams **3a**−**d** were prepared in excellent yields through the acylation of enantiopure β-lactams **1a**,**b** with the corresponding 2-alkenylbenzoyl chlorides **2a**−**c**[34−36] in the presence of triethylamine and DMAP. 7-TES-14β-allyloxybaccatin **6** was prepared following the method previously reported by us from 14-OH-DAB through selective acetylation of the C10-hydroxyl group[37] and subsequent TES protection of the C7-hydroxyl group (83% for two steps, Scheme 3).[8] The Ojima−Holton coupling of β-lactams **3a**−**d** with baccatin **6** was carried out under the standard conditions (LiHMDS in THF at −30 °C) to give the corresponding paclitaxel-dienes **7a**−**d** bearing olefinic groups at the C14 position as well as the *ortho* position of the C3′BzN moiety (Scheme 3).

As Scheme 4 shows, the RCM reactions of paclitaxel-dienes **7a** and **7d** catalyzed by the "1st-generation Grubbs catalyst", $Cl_2Ru(=CHPh)(PCy_3)_2$, proceeded smoothly at room temperature to give the corresponding macrocyclic taxoids **8a** and **8d**, respectively, which were isolated in high yields by passing through a short silica gel column to remove the Ru catalyst. The crude **8a** and **8d**, thus obtained, were subjected to the deprotection of all silyl groups with HF−pyridine to give the designed macrocyclic taxoids **1a** and **1d**, respectively, in high yields. In both products, *E*-isomer was formed exclusively. We reported the synthesis of **1a** (SB-T-2053) in 2005,[8] but we needed to resynthesize this macrocyclic taxoid for additional cytotoxicity assay for comparison purposes. We confirmed that the reported synthesis is perfectly reproducible.

The RCM reaction of **7c** proceeded slowly at room temperature. Thus, the reaction mixture was heated at reflux for 3 days until **7c** had disappeared. The reaction gave *E* and *Z* isomers at the alkene moiety formed, i.e., **8c-*E*** and **8c-*Z***, in 40% and 42% yields, respectively. The observed low reactivity of **7c** and the lack of stereoselectivity in the alkene formation can be attributed to the larger ring size of the product(s). The silyl groups of **8c-*E*** and **8c-*Z*** were removed by HF−pyridine to give **1c-*E*** and **1c-*Z***, respectively, in high yields (Scheme 5).

In contrast to the RCM reactions described above, the reaction of paclitaxel-diene **7b** did not proceed as anticipated. The attempted RCM reaction of **7b** was sluggish. Thus, the reaction was run in refluxing dichloromethane for 5 days. As often observed in RCM reactions, deactivation of the Ru catalyst appeared to have occurred. Accordingly, more Ru catalyst was added during the reaction (0.25 equiv × 3). The reaction stopped at 75% conversion (i.e., 25% of the unreacted **7c** was recovered), giving ring-closed product **8b** in 50% yield. Then, the silyl groups were removed by HF−pyridine to give the corresponding macrocyclic taxoid **9b** in high yield. However, the LCMS analysis of **9b** showed its molecular weight higher than the anticipated RCM product **1b** by 14 mass units, which was quite puzzling. The ^{1}H and ^{13}C NMR and 2D NMR analyses

(27) Ojima, I.; Slater, J. C.; Michaud, E.; Kuduk, S. D.; Bounaud, P.-Y.; Vrignaud, P.; Bissery, M.-C.; Veith, J.; Pera, P.; Bernacki, R. J. *J. Med. Chem.* **1996**, *39*, 3889–3896.
(28) Ojima, I.; Chen, J.; Sun, L.; Borella, C. P.; Wang, T.; Miller, M. L.; Lin, S.; Geng, X.; Kuznetsova, L. V.; Qu, C.; Gallager, D.; Zhao, X.; Zanardi, I.; Xia, S.; Horwtiz, S. B.; Mallen-St. Clair, J.; Guerriero, J. L.; Bar-Sagi, D.; Veith, J. M.; Pera, P.; Bernacki, R. J. *J. Med. Chem.* **2008**, *51*, 3203–3221.
(29) Grubbs, R. H.; Chang, S. *Tetrahedron* **1998**, *54*, 4413–4450.
(30) Ojima, I.; Habus, I.; Zhao, M.; Zucco, M.; Park, Y. H.; Sun, C. M.; Brigaud, T. *Tetrahedron* **1992**, *48*, 6985–7012.
(31) Ojima, I. *Acc. Chem. Res.* **1995**, *28*, 383–389, and references cited therein.
(32) Ojima, I.; Chakravarty, S.; Inoue, T.; Lin, S.; He, L.; Horwitz, S. B.; Kuduk, S. D.; Danishefsky, S. J. *Proc. Natl. Acad. Sci. U.S.A.* **1999**, *96*, 4256–4261.
(33) Ojima, I.; Geng, X.; Lin, S.; Pera, P.; Bernacki, R. J. *Bioorg. Med. Chem. Lett.* **2002**, *12*, 349–352.
(34) Reich, S. H.; Melnick, M.; Pino, M. J.; Fuhry, M. A. M.; Trippe, A. J.; Appelt, K.; Davies, J. F.; Wu, B. W.; Musick, L. *J. Med. Chem.* **1996**, *39*, 2781–2794.
(35) Chang, S.; Grubbs, R. H. *J. Org. Chem.* **1998**, *63*, 864–866.
(36) Kim, B. M.; Park, J. K. *Bull. Korean Chem. Soc.* **1999**, *20*, 744–746.
(37) Holton, R. A.; Zhang, Z.; Clarke, P. A.; Nadizadeh, H.; Procter, D. J. *Tetrahedron Lett.* **1998**, *39*, 2883–2886.

SCHEME 1. Retrosynthetic Analysis of the Designed Macrocyclic Taxoids 1a−c

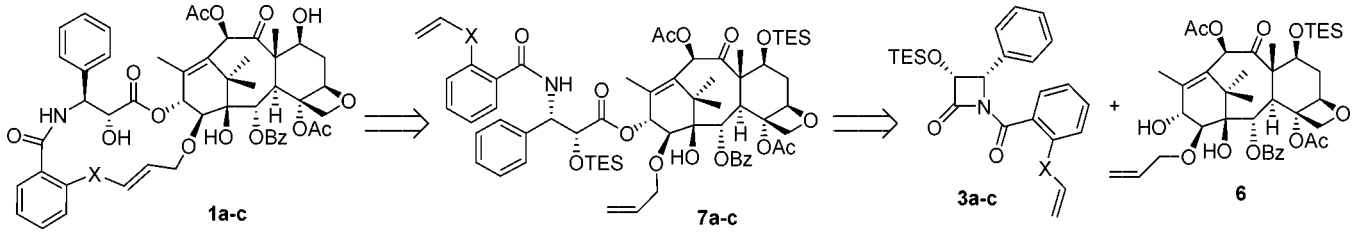

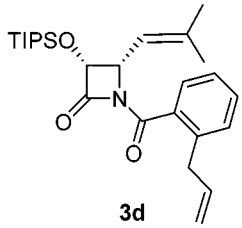

SCHEME 2[a]

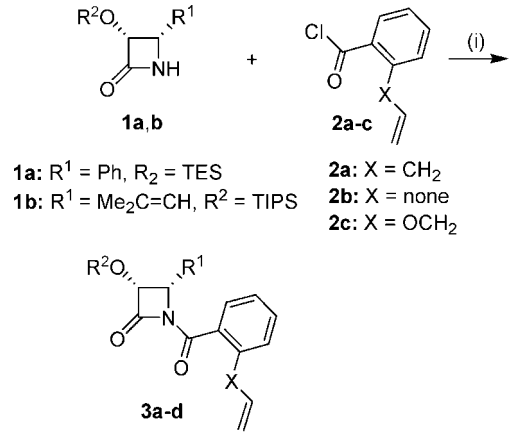

[a] Reagents and conditions: (i) acid chloride (2.0 equiv), Et_3N (4 equiv), CH_2Cl_2, DMAP, overnight.

SCHEME 3[a]

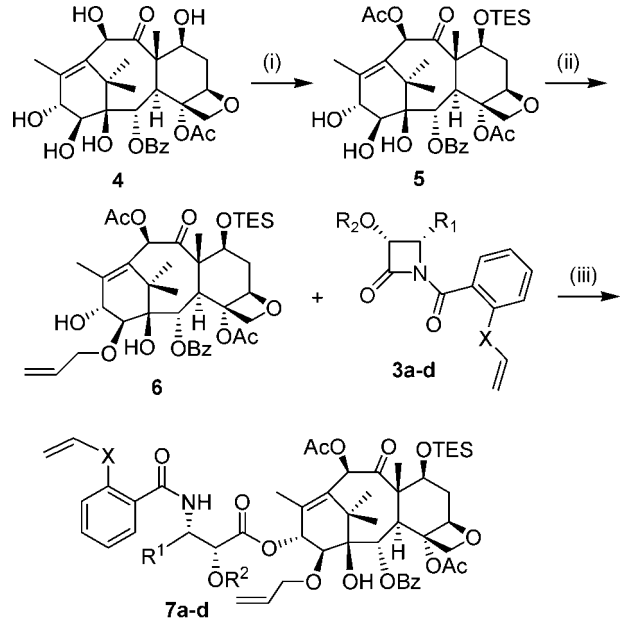

[a] Reagents and conditions: (i) (a) Ac_2O (10 equiv), $CeCl_3 \cdot 7H_2O$ (0.1 equiv), THF, rt, 2 h, (b) TESCl (3.0 equiv), imidazole (4.0 equiv), DMF, rt, 5 h (83% in 2 steps), (ii) allyl iodide (1.1 equiv), NaHMDS (1.1 equiv), DMF, −40 °C, 1 h (82%), (iii) **3a−d** (3.0 equiv), LiHMDS (1.5 equiv), THF, −30 to 0 °C, 2.5 h.

suggested that **9b** should possess a butenylene unit between the C14−O and the *ortho* position of the C3′*N*-benzoyl moiety and the newly formed double bond should be conjugated to the phenyl group. This proposed structure was confirmed by the X-ray crystallographic analysis of **9b** (SB-T-2054) as shown in Figure 4. This unexpected reaction is shown in Scheme 6.

A plausible mechanism for this unique reaction is proposed in Scheme 7. The first step of this process would be the formation of a Ru−carbene intermediate **M-1** through a normal Ru−carbene exchange reaction. In the next step, however, a normal metalacyclobutane intermediate **M-2** is not formed, which is very likely due to the macrocyclic ring strain for the formation of a 14-membered ring. Since **M-2** is the precursor of the RCM product **diTES-1b**, the expected RCM reaction is blocked at this stage. Instead, regioisomeric metalacyclobutane intermediate **M-3** is generated, forming a 15-membered ring. There are two possible pathways from **M-3**, i.e., (i) reductive elimination to form a cyclopropane **10** or (ii) ring-opening through β-hydride elimination to form a σ-allylic Ru intermediate **M-5a** and/or its regioisomer **M-5b**, which may well be equilibrated via π-allylic Ru intermediate **M-5**. Apparently, the first pathway did not happen since the formation of cyclopropane product **10** was not observed. Thus, the reaction should have proceeded through the possible pathway (ii). Since **M-5a** has a clear stabilization through double-bond conjugation to the benzene ring, the reaction gives thermodynamically favorable product **8b** through reductive elimination. To the best of our knowledge, this is the first example of a unique ring-closing olefin−olefin coupling reaction promoted by the Grubbs RCM catalyst.

SCHEME 4[a]

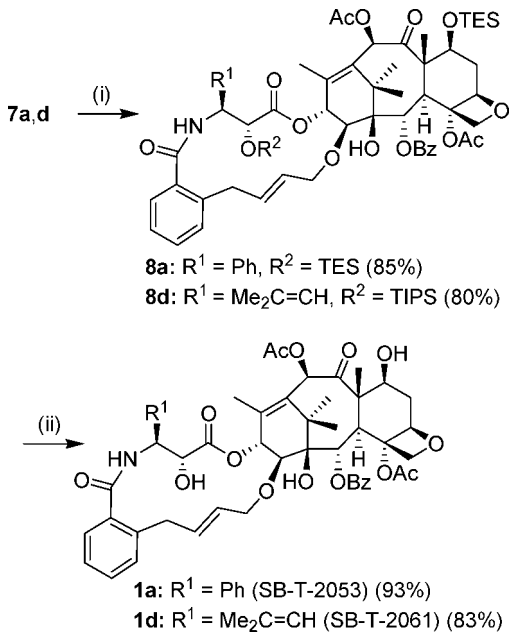

[a] Reagents and conditions: (i) (a) $Cl_2Ru(=CHPh)(PCy_3)_2$ (0.2 equiv), CH_2Cl_2, overnight; (ii) HF/Py, Py, CH_3CN, rt, overnight.

SCHEME 5[a]

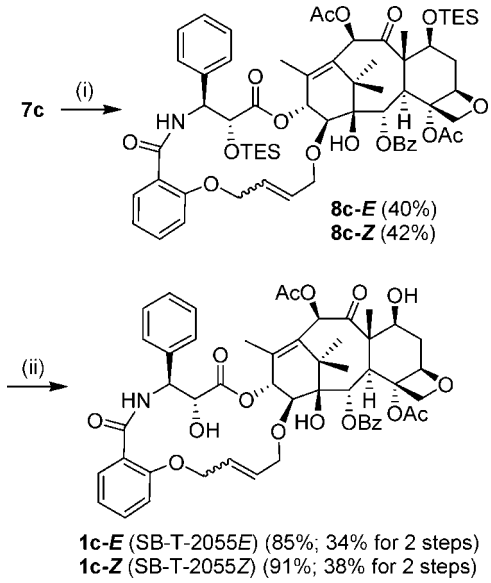

[a] Reagents and conditions: (i) (a) $Cl_2Ru(=CHPh)(PCy_3)_2$ (0.2 equiv), CH_2Cl_2, overnight, flash chromatography; (ii) HF/Py, Py, CH_3CN, rt, overnight.

It should be noted that this Ru−carbene complex promoted reaction does not regenerate the living Ru−carbene complex, different from RCM reactions, since the final step in this process is the reductive elimination of the alkene product **8b** and Ru(II) species without a carbene bond. The fact that 75% conversion was attained by using 0.75 equiv (total) of $Cl_2Ru(=CHPh)(PCy_3)_2$ may indicate that the reaction proceeded very well as it should, although we did not recognize it at the time of the experiment.

Evaluation of Biological Activities. Cytotoxicity of Macrocyclic Taxoids against Human Breast, Ovarian, And Colon Cancer Cell Lines. Novel macrocyclic taxoids, thus obtained, were evaluated for their cytotoxicity against drug-sensitive and drug-resistant human breast cancer cell lines, drug-resistant human ovarian cancer cell line, as well as drug-sensitive human colon and overian cancer cell lines. The results are summarized in Table 1.

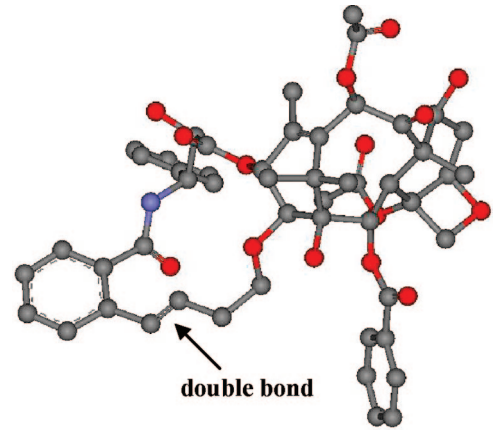

FIGURE 4. X-ray crystal structure of **9b** (SB-T-2054).

SCHEME 6[a]

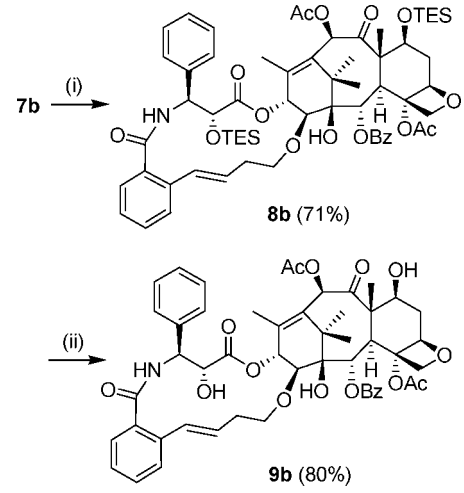

[a] Reagents and conditions: (i) (a) $Cl_2Ru(=CHPh)(PCy_3)_2$ (0.25 equiv × 3), CH_2Cl_2, reflux, 5d; (ii) HF/Py, Py, CH_3CN, rt, overnight.

As Table 1 shows, **9b** (SB-T-2054) is the most potent compound among the macrocyclic taxoids synthesized and evaluated. It is worthy of note that the potency of **9b** is almost equivalent to that of paclitaxel against all six cell lines; i.e., **9b** is more potent than paclitaxel against NCI/ADR, LCC6-WT, and A2780 cell lines but less potent than paclitaxel against MCF7, LCC6-MDR, and HT-29. The results may suggest that **9b** is very closely mimicking paclitaxel's bioactive conformation. This is also confirmed by the tubulin polymerization assay described below. Macrocyclic taxoid **1a** (SB-T-2053) is an olefin regioisomer of **9b**, which is 2−3 times less potent than **9b**. The results appear to indicate high sensitivity of the potency to the subtle difference in the position of C3′N-benzoyl group and the rigidity of the macrocyclic structure. Larger ring analogues **1c-*E*** and **1c-*Z*** exhibit substantial loss of potency. Also, there is a marked difference between the *E* isomer and the *Z* isomer, wherein the *Z* isomer (**1c-*Z***) is 6−8 times more potent than the *E* isomer, except for the LCC6-MDR cell line. The result further indicates the highly delicate effects of ring size and rigidity of the macrocyclic taxoids on their potency. Macrocyclic taxoid **1d**, which is a 3′-(2-methylpropen-2-yl) analogue of **1a**, shows 2−30 times less potency than **1a**. This result is a surprise for

SCHEME 7. Plausible Mechanism for the Formation of 8d via Novel Ring-Closing Coupling

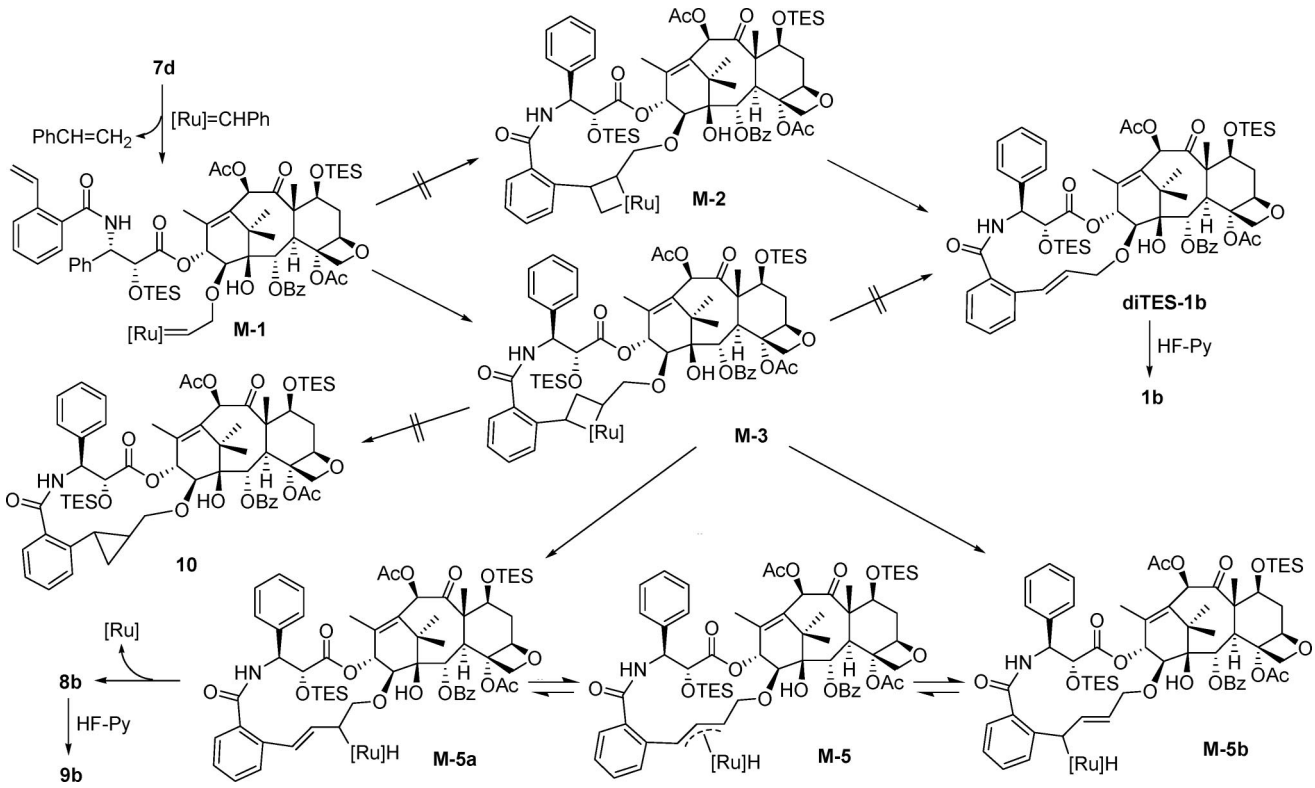

TABLE 1. Cytotoxicity of C14−C3′BzN-Linked Macrocyclic Taxoids (IC_{50} nM)[a]

taxoids	MCF-7[b]	NCI/ ADR[c]	LCC6-WT[d]	LCC6-MDR[e]	A2780[f]	HT-29[g]
paclitaxel	1.85	395	2.45	110	36.1	7.28
1a	12.3	592	12.2	300	114	29.2
9b	3.49	183	2.09	129	31.0	17.0
1c-*E*	1,650	10,010	2,067	2,285	1,475	523
1c-*Z*	196	1,135	348	1,924	198	62.0
1d	398	1,000	130	618		

[a] Concentration of compound which inhibits 50% (IC_{50}, nM) of the growth of human tumor cell line after 72 h drug exposure. [b] MCF7: human breast carcinoma cell line. [c] NCI/ADR: multidrug resistant human ovarian carcinoma cell line. [d] LCC6-WT: human breast carcinoma cell line (Pgp-). [e] LCC6-MDR: *mdr1*-transduced cell line (Pgp+). [f] A2780 human ovarian carcinoma cell line. [g] HT-29 human colon carcinoma cell line.

us since the replacement of the 3′-phenyl moiety of paclitaxel and docetaxel with a 2-methylpropen-2-yl group has been shown to increase the potency.[27,28] Thus, the result may suggest that the second-generation taxoids bearing 3′-(2-methylpropen-2-yl) moiety have a slightly different binding site from that of paclitaxel or these taxoids have a different bioactive conformation that that of paclitaxel.

Microtubule Polymerization Assay. The activity of **9b** (SB-T-2054) was evaluated in in vitro tubulin polymerization assay. Paclitaxel was used as the standard for comparison. Changes in absorbance in this spectrophotometric assay provide the direct measure of turbidity, hence indicating the extent of tubulin polymerization. As Figure 5 shows, **9b** induced tubulin polymerization in the absence of GTP in a manner similar to that of paclitaxel. The microtubules formed with **9b** as well as paclitaxel were stable against Ca^{2+}-induced depolymerization. We have already reported that **1a** (SB-T-2053) also exhibited virtually the same or slightly better activity than that of paclitaxel in the same assay.[8] This result also supports our observation that **9b** is closely mimicking paclitaxel's bioactive conformation, as mentioned above.

Electron Microscopy Analysis. The microtubules formed with **9b** were analyzed further by electron microscopy for their morphology and structure in comparison with those formed by using GTP and paclitaxel. As Figure 6 shows, the microtubules formed with **9b** and paclitaxel are very similar, while those formed with GTP are longer and more uniform.

Molecular Modeling Analysis. The microtubule-bound structure of **9b** (SB-T-2054) was energy minimized in the 1JFF coordinate and overlaid with the "REDOR-Taxol" structure in the 1JFF β-tubulin. The overlay of **9b** with the "REDOR-Taxol" is shown in Figure 7. The H-bond between the C2′-OH of **9b** and His^{227} is 2.7 Å.

Figure 8 shows the overlay of **9b** with **1a** (SB-T-2053). Those two structures are very close, but there is a slight difference in the position of the C3′*N*-benzoyl group as well as the rigidity of the macrocyclic structure; i.e., **9b** is more rigid than **1a**, due to the conjugation of the ethenyl group to the benzoyl group.

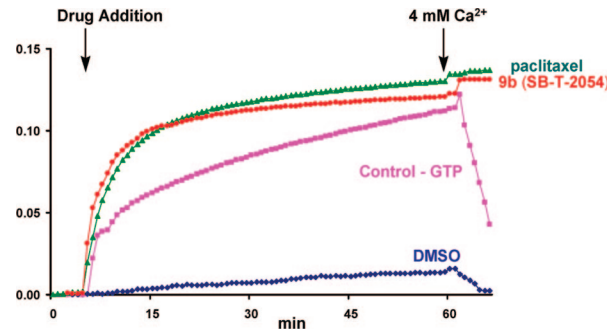

FIGURE 5. Tubulin polymerization with **9b** and paclitaxel: microtubule protein 1 mg/mL, 37 °C, GTP 1 mM, drug 10 μM.

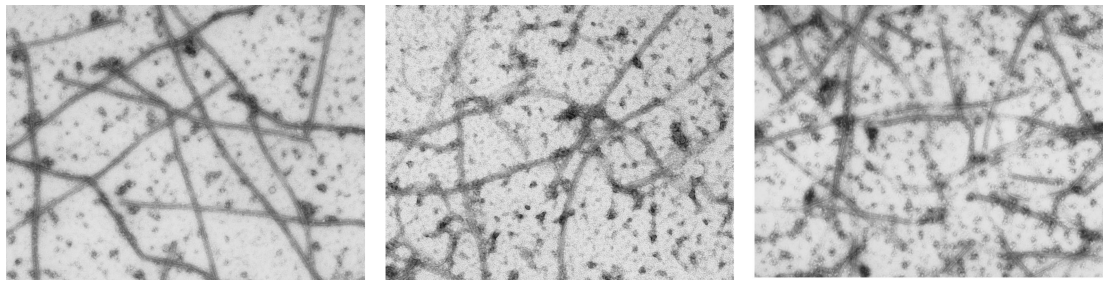

FIGURE 6. Electromicrographs of microtubule: (a) GTP, (b) paclitaxel, and (c) **9b** (SB-T-2054).

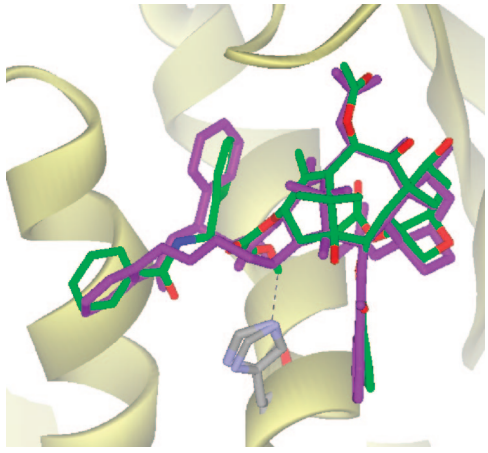

FIGURE 7. Overlays of REDOR-Taxol (green) with **9b** (SB-T-2054) (purple).

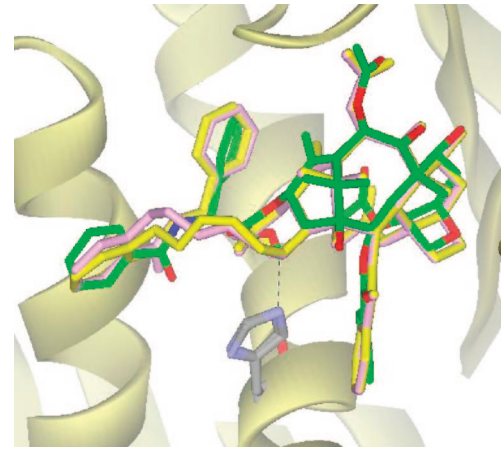

FIGURE 9. Overlay of REDOR-Taxol (green) with **1c-*E*** (pink) and **1c-*Z*** (yellow).

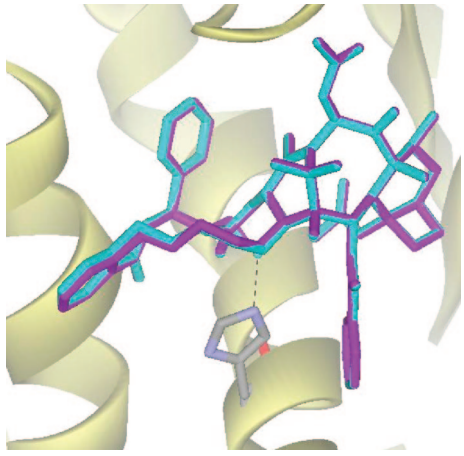

FIGURE 8. Overlay of **9b** (purple) and **1a** (SB-T-2053) (cyan).

These subtle differences appear to be correlated to the 2−3 times difference in their potency,

Figure 9 shows the overlay of **1c-*E***, **1c-*Z***, and the "REDOR-Taxol". As the cytotoxicity assay revealed (see Table 1), there is a 6−8 times difference in the potency of these two stereoisomers; i.e., **1c-*Z*** is substantially more potent than **1c-*E***. It is clear that **1c-*Z*** has a C3′*N*-benzoyl group orientation closer to that of **1a** and **9b** as compared to that of **1c-*E*** and **1c-*Z*** is more rigid than **1c-*E***. Monte Carlo conformational analysis of **1c-*E*** and **1c-*Z*** in a simulated aqueous environment supports the substantial difference in the rigidity of these two stereoisomes (see the Supporting Information).

We also performed the Monte Carlo conformational analysis of **9b** and **1c** under the same conditions. We started from their "REDOR-Taxol" conformation as well as "T-Taxol" conformation, but both converged to the same distribution of conformers (see the Supporting Information). The results indicate that the X-ray crystal structure of **9b** (see Figure 5) is just one of the preferred conformations in a crystalline state. Also, the dihedral angle of C13−C1′−C2′−O2′ of **9b** does not match those of the "REDOR-Taxol" and the "T-Taxol", which may suggest that both proposed bioactive conformations of paclitaxel need further refinements.

In summary, novel C14−C3′BzN-linked macrocyclic taxoids **1a** (SB-T-2053), **1c-*E***, **1c-*Z***, **1d**, and **9b** (SB-T-2054) were synthesized based on the computational design, mimicking the "REDOR-Taxol" structure. The Ru-catalyzed RCM reaction was employed in the key macrocyclization step of the paclitaxel-dienes **7a**−**d**. The formation of 15- and 16-membered macrocyclic taxoids (**1a**, **1c**, and **1d**) proceeded as anticipated, while that of 14-membered macrocyclic taxoid **1b** did not go through. However, a novel Ru-catalyzed intramolecular coupling of two ethenyl moieties was discovered instead, which gave 15-membered macrocyclic taxoid **9b** (SB-T-2054). This new process is likely to involve a metalacyclobutane intermediate, regioisomeric to the RCM intermediate, followed by β-hydride elimination and reductive elimination. Evaluation of the biological activities of these novel macrocyclic taxoids has revealed that their potency is highly sensitive to the subtle conformational differences as well as the rigidity of the compounds. Computational analysis for the structure−activity relationships of these novel macrocyclic taxoids is consistent with this observation. Macrocyclic taxoid **9b** is found to be the most potent compound among those synthesized and assayed. It is noteworthy that **9b** exhibits virtually the same potency as that of paclitaxel in the cytotoxicity and tubulin-polymerization assays as well as morphology analysis of microtubules by electron microscopy, which may indicate that **9b** structure almost perfectly mimics the bioactive conformation of paclitaxel.

Experimental Section

General Methods. ^{1}H and ^{13}C NMR spectra were measured on a Varian 300, 400, 500, or 600 MHz NMR spectrometer or a Bruker AC-250 NMR spectrometer. Melting points were measured on a Thomas-Hoover Capillary melting point apparatus and are uncorrected. Specific optical rotations were measured on a Perkin-Elmer Model 241 polarimeter. IR spectra were recorded on a Perkin-Elmer Model 1600 FT-IR spectrophotometer. TLC was performed on Merck DC-alufolien with Kieselgel 60F-254, and column chromatography was carried out on silica gel 60 (Merck; 230−400 mesh ASTM). Purity was determined with a Waters HPLC assembly consisting of dual Waters 515 HPLC pumps, a PC workstation running Millennium 32, and a Waters 996 PDA detector, using a Phenomenex Curosil-B column, employing CH_3CN/water (2/3) as the solvent system with a flow rate of 1 mL/min. High-resolution mass spectra were obtained at the Mass Spectrometry Laboratory, University of Illinois at Urbana−Champaign, Urbana, IL, or the Mass Spectrometry Facility, University of California, Riverside, CA.

Materials. The chemicals were purchased from a commercial supplier and used as received or purified before use by standard methods. Tetrahydrofuran was freshly distilled from sodium metal and benzophenone. Dichloromethane was also distilled immediately prior to use under nitrogen from calcium hydride. *N,N*-Dimethylformamide (DMF) was distilled over 4A molecular sieves under reduced pressure. 4-(*N,N*-Dimethylamino)pyridine (DMAP) was used as received. 14β-Hydroxyl-deacetylbaccatin III (DAB, **4**) was obtained from a commercial supplier. (3*R*,4*S*)-3-Triethylsiloxy-4-phenylazetidin-2-one (**1a**)[15] and (3*R*,4*S*)-3-*tert*-butyldimethylsiloxy-4-(2-methylpropen-2-yl)azetidin-2-one (**1b**)[27] were prepared by the methods we reported. (3*R*,4*S*)-1-(2-Allylbenzoyl)-3-triethylsiloxy-4-phenylazetidin-2-one (**3a**), 7-triethylsilyl-14β-hydroxybaccatin III (**5**), 14β-allyloxy-3′*N*-debenzoyl-3′*N*-(2-allylbenzoyl)-7,2′-triethylsilylpaclitaxel (**7a**), and macrocyclic taxoid **1a** (SB-T-2053) were synthesized using our methods previously reported.[8]

1-(2-Alkenylbenzoyl)-β-lactams (3a−d). The procedure for the synthesis of β-lactam **3d** is described as a typical example. To a solution of (3*R*,4*S*)-3-triisopropylsiloxy-4-phenylazetidin-2-one (**1b**) (106 mg, 0.365 mmol), triethylamine (0.2 mL, 1.46 mmol), and DMAP (8 mg, 0.073 mmol) in CH_2Cl_2 (2 mL) was added 2-allylbenzoyl chloride (**2a**) (2 equiv) in a solution of CH_2Cl_2 (2 mL) dropwise at room temperature. The mixture was stirred overnight at room temperature, and the reaction was quenched with saturated aqueous NH_4Cl solution (2 mL). The mixture was then extracted with CH_2Cl_2 (10 mL × 3). The combined extracts were dried over anhydrous $MgSO_4$ and concentrated in vacuo. The crude product was purified on a silica gel column using hexanes/EtOAc (9/1) as the eluent to afford (3*R*,4*S*)-1-(2-allylbenzoyl)-3-triisopropylsiloxy-4-(2-methylprop-1-enyl)azetidin-2-one (**3d**) as a colorless oil (126 mg, 80% yield): ^{1}H NMR (300 MHz, $CDCl_3$) δ 0.99 (m, 21 H), 1.81 (br s, 6 H), 3.42−3.61 (m, 2 H), 4.98−5.04 (m, 4 H), 5.36 (d, J = 8.2 Hz, 1 H), 5.87−6.01 (m, 1 H), 7.27 (m, 2 H), 7.37 (m, 1 H), 7.50 (m, 1 H); ^{13}C NMR (75.0 MHz, $CDCl_3$) δ 12.2, 17.4, 18.3, 26.0, 37.3, 56.3, 116.0, 117.7, 125.8, 128.5, 129.9, 131.4, 133.6, 136.8, 138.4, 140.4, 165.6, 166.7. HRMS (EI) *m*/*z* calcd for $C_{26}H_{39}NO_3SiH^+$ 442.2777, found 442.2776 (Δ = 0.1 ppm).

In a similar manner, β-lactams **3a**−**c** were prepared from (3*R*,4*S*)-3-triethylsiloxy-4-phenylazetidin-2-one (**1a**) (for **3a**, see Materials, vide supra).

(3*R*,4*S*)-1-(2-Ethenylbenzoyl)-3-triethylsiloxy-4-phenylazetidin-2-one (3b): colorless oil; ^{1}H NMR (600 MHz, $CDCl_3$) δ 0.44 (m, 6 H), 0.77 (m, 9 H), 5.15 (d, J = 6.6 Hz, 1 H), 5.33 (m, 2 H), 5.69 (d, J = 17.4 Hz, 1 H), 6.94 (dd, J = 17.4, 10.8 Hz, 1 H), 7.33 (m, 6 H), 7.47 (m, 1 H), 7.52 (m, 1 H), 7.59 (d, J = 6.8 Hz, 1 H); ^{13}C NMR (100.5 MHz, $CDCl_3$) δ 4.3, 6.16, 61.4, 76.9, 117.3, 126.1, 127.2, 128.1, 128.1, 128.3, 128.5, 131.3, 132.1, 133.5, 133.8, 136.9, 165.3, 166.4; HRMS (FAB/DCM/NaCl) *m*/*z* calcd for $C_{24}H_{29}NO_3SiH^+$ 408.1995, found 408.1995 (Δ = 0 ppm).

(3*R*,4*S*)-1-(2-Allyloxybenzoyl)-3-triethylsiloxy-4-phenylazetidin-2-one (3c): colorless oil; ^{1}H NMR (300 MHz, $CDCl_3$) δ 0.40−0.50 (m, 6 H), 0.75−0.81 (m, 9 H), 4.62 (dd, J = 5.7, 1.2 Hz, 2 H), 5.10 (d, J = 6.0 Hz, 1 H), 5.22 (dd, J = 10.5, 0.9 Hz, 1 H), 5.36 (d, J = 6.0 Hz, 1 H), 5.45 (dd, J = 17.4, 1.8 Hz, 1 H), 6.04−6.20 (m, 1 H), 6.96−7.03 (m, 2 H), 7.32−7.45 (m, 7 H); ^{13}C NMR (75 Hz, $CDCl_3$) δ 4.34, 6.15, 61.5, 69.7, 70.1, 112.2, 118.3, 120.5, 124.2, 127.8, 127.9, 128.0, 129.4, 132.8, 132.9, 133.6, 156.9, 164.6, 165.0; HRMS (FAB/DCM/NaCl) *m*/*z* calcd for $C_{25}H_{31}NO_4SiH^+$ 438.2100, found 438.2088 (Δ = −2.7 ppm).

14β-Allyloxy-7-triethylsilylbaccatin III (6). To a solution of **5** (427 mg, 0.596 mmol) in DMF (20 mL) was added 1.0 M sodium bis(trimethylsilyl)amide (NaHMDS) in THF (0.656 mL, 0.656 mmol) at −40 °C, the reaction mixture was stirred for 5 min, and then allyl iodide (0.060 mL, 0.656 mmol) was added. The reaction was quenched after 10 min with saturated aqueous NH_4Cl (5 mL). The reaction mixture was extracted with ethyl acetate (100 mL) and washed with water (10 mL × 3) and brine (10 mL). The organic layer was dried over anhydrous $MgSO_4$ and filtered, and the solvent was removed under reduced pressure. The residue was purified on a silica gel column using hexanes/EtOAc (6/1) as the eluant to afford **6** as a white solid (361 mg, 80%): mp 133−135 °C; ^{1}H NMR (300 MHz, $CDCl_3$) δ 0.55 (m, 6 H), 0.90 (m, 9 H), 1.19 (s, 3 H), 1.60 (m, 2 H), 1.66 (s, 3 H), 1.84 (m, 1 H), 2.00 (m, 3 H), 2.12 (s, 3 H), 2.29 (s, 3 H), 2.50 (m, 1 H), 3.22 (d, J = 4.2 Hz, 1 H), 3.69 (d, J = 5.7 Hz, 1 H), 3.77 (m, 2 H), 4.06 (m, 1 H), 4.18 (m, 1 H), 4.29−4.47 (m, 3 H), 4.69 (bs, 1 H), 4.87−4.98 (m, 3 H), 5.61−5.72 (m, 1 H), 5.83 (d, J = 6.9 Hz, 1 H), 7.42 (m, 2 H), 7.55 (m, 1 H), 8.06 (m, 2 H); ^{13}C NMR (62.9 MHz, $CDCl_3$) δ 5.1, 5.4, 6.6, 6.7, 9.7, 10.0, 14.7, 20.8, 21.4, 22.4, 26.2, 37.1, 42.7, 46.4, 58.7, 72.1, 73.0, 74.5, 75.6, 75.7, 76.2, 76.4, 80.9, 81.5, 82.0, 84.0, 117.4, 128.4, 129.7, 129.8, 133.3, 133.6, 133.7, 141.2, 165.6, 169.3, 170.1, 201.9; HRMS (FAB/DCM/NaCl) *m*/*z* calcd for $C_{40}H_{56}O_{12}SiH^+$ 757.3619, found 757.3643 (Δ = −3.1 ppm).

7,2′-Disilylpaclitaxel-diene Analogues 7a−d, Substrates for RCM Reactions. The procedure for the synthesis of **7d** is described as a typical example (for **7a**, see Materials, vide supra). To a solution of **6** (100 mg, 0.13 mmol) and β-lactam **3d** (3 equiv) in THF (15 mL) was added 1 M LiHMDS in THF (0.2 mL, 0.20 mmol) at −40 °C. The reaction mixture was warmed to −20 °C over 1 h and then quenched with saturated aqueous NH_4Cl solution (10 mL) and extracted with EtOAc (30 mL × 3). The organic layers were combined, and solvent was removed by reduced pressure vacuum. The residue was purified by using chromatography column on silica gel using hexanes/EtOAc (9/1) to afford 7-triethylsilyl-14β-allyloxy-2′-triisopropyl-3′-dephenyl-3′-(2-methylprop-1-enyl)-3′*N*-debenzoyl-3′*N*-(2-allylbenzoyl)paclitaxel (**7d**) as a white solid (115 mg, 73%): ^{1}H NMR (300 MHz, $CDCl_3$) δ 0.60−0.65 (m, 6 H), 0.93−1.00 (m, 9 H), 1.18 (s, 21 H), 1.32 (s, 3 H), 1.77 (s, 3 H), 1.83 (s, 3 H), 1.91−2.03 (m, 3 H), 1.92 (s, 3 H), 2.05 (s, 3 H), 2.20 (s, 3 H), 2.43 (s, 3 H), 2.50−2.54 (m, 1 H), 3.45−3.61 (m, 2 H), 3.74 (s, 1 H), 3.84 (m, 2 H), 3.92−3.98 (m, 1 H), 4.30−4.32 (d, J = 8.4 Hz, 1 H), 4.43−4.58 (m, 3 H), 4.69 (s, 1 H), 4.79 (d, J = 9.9 Hz, 1 H), 4.94−5.09 (m, 3 H), 5.14−5.20 (m, 1 H), 5.45 (d, J = 9.0 Hz, 1 H), 5.67−5.81 (m, 1 H), 5.91−6.11 (m, 3 H), 6.48−6.51 (m, 2 H), 7.22−7.26 (m, 2 H), 7.30−7.54 (m, 5), 8.14−8.16 (m, 2 H); ^{13}C NMR (62.9 MHz, $CDCl_3$) δ 5.3, 6.7, 9.8, 12.6, 14.5, 17.9, 18.1, 18.7, 20.1, 22.7, 25.7, 26.1, 37.2, 43.3, 46.0, 50.8, 58.7, 72.2, 72.5, 74.5, 75.0, 75.1, 76.4, 78.7, 78.9, 81.6, 84.1, 115.8, 118.2, 122.2, 126.2, 127.3, 128.5, 129.6, 129.9, 130.1, 133.0, 133.4, 135.4, 136.0, 136.2, 136.4, 137.4, 137.9, 165.5, 168.5, 169.3, 171.3, 172.0, 201.1; HRMS calcd. for $C_{66}H_{95}NO_{15}Si_2H^+$ 1198.6318, found 1198.6320 (Δ= −0.1 ppm).

14β-Allyloxy-3′*N*-debenzoyl-3′*N*-(2-ethenylbenzoyl)-7,2′-triethylsilylpaclitaxel (7b): white solid; mp 99−102 °C; $[\alpha]^{20}_D$ −42 (*c* 0.6, $CHCl_3$); ^{1}H NMR (600 MHz, $CDCl_3$) δ 0.34−0.47 (m, 6 H), 0.55−0.63 (m, 6 H), 0.78 (m, 9 H), 0.93 (m, 9 H), 1.15 (s, 3 H), 1.31 (s, 3 H), 1.74 (s, 3 H), 1.95 (m, 1 H), 2.03 (s, 3 H), 2.19 (s, 3 H), 2.56 (m, 1 H), 2.60 (s, 3 H), 3.67 (s, 1 H), 3.82 (d, J =

7.2 Hz, 1 H), 3.84 (d, J = 8.0 Hz, 1 H), 3.93 (dd, J = 10.8, 4.2 Hz, 1 H), 4.28 (d, J = 9.0 Hz, 1 H), 4.32 (dd, J = 10.5, 4.0 Hz, 1 H), 4.47 (m, 3 H), 4.62 (d, J = 10.5 Hz, 1 H), 4.71 (d, J = 1.2 Hz, 1 H), 5.00 (d, J = 9.0 Hz, 1 H), 5.32 (d, J = 7.6 Hz, 1 H), 5.36 (m, 1 H), 5.61 (d, J = 8.4 Hz, 1 H), 5.70 (d, J = 11.4 Hz, 1 H), 5.99 (d, J = 7.8 Hz, 1 H), 6.21 (d, J = 7.0 Hz, 1 H), 6.47 (s, 1 H), 6.99 (m, 2 H), 7.26−7.48 (m, 8 H), 7.50−7.58 (m, 3 H), 8.10 (d, J = 8.4 Hz, 2 H); ^{13}C NMR (75.5 MHz, $CDCl_3$) δ 4.3, 5.3, 6.4, 6.7, 9.9, 14.4, 20.8, 23.3, 26.1, 37.3, 43.5, 45.9, 56.1, 58.8, 72.3, 72.5, 74.8, 74.9, 76.5, 76.6, 78.6, 78.6, 81.7, 84.1, 117.2, 117.8, 126.3, 126.5, 127.7, 128.0, 128.7, 129.5, 129.9, 130.6, 132.7, 133.5, 134.2, 134.8, 135.6, 136.2, 136.5, 138.6, 165.6, 168.3, 169.4, 169.7, 171.4, 201.0; HRMS (FAB/DCM/NaCl) *m/z* calcd for $C_{64}H_{85}NO_{15}Si_2H^+$ 1164.5536, found 1164.5535 (Δ = 0.1 ppm).

14β-Allyloxy-3′*N*-debenzoyl-3′*N*-(2-allyloxybenzoyl)-7,2′-triethylsilylpaclitaxel (7c): white solid; ^{1}H NMR (400 MHz, $CDCl_3$) δ 0.28−0.48 (m, 6 H), 0.52−0.66 (m, 6 H), 0.76−0.86 (m, 9 H), 0.88−0.98 (m, 9 H), 1.11 (s, 3 H), 1.25 (s, 3 H), 1.73 (s, 3 H), 1.88−1.98 (m, 1 H), 2.01 (s, 3 H), 2.17 (s, 3 H), 2.50−2.60 (m, 1 H), 2.66 (s, 3 H), 3.74 (s, 1 H), 3.76−3.88 (m, 3 H), 4.20 (dd, J = 10.8, 4.4 Hz, 1 H), 4.28 (d, J = 8.4 Hz, 1 H), 4.42−4.55 (m, 4 H), 4.70 (d, J = 1.6 Hz, 1 H), 4.74−4.83 (dd, J = 13.2, 5.2 Hz, 1 H), 4.83−4.89 (dd, J = 12.8, 5.6 Hz, 1 H), 5.0 (d, J = 8.4 Hz, 1 H), 5.20−5.30 (m, 1 H), 5.34 (d, J = 10.4 Hz, 1 H), 5.44 (d, J = 16.4 Hz, 1 H), 5.64 (d, J = 6.4 Hz, 1 H), 5.96 (d, J = 7.2 Hz, 1 H), 6.16−6.30 (m, 2 H), 6.45 (s, 1 H), 6.92−7.0 (m, 2 H), 7.26−7.42 (m, 6 H), 7.48 (t, J = 7.2 Hz, 2 H), 7.59 (t, J = 7.6 Hz, 1 H), 8.02 (dd, J = 1.6, 8 Hz, 1 H), 8.10 (d, J = 7.2 Hz, 2 H), 9.09 (d, J = 7.6 Hz, 1 H); ^{13}C NMR (100 MHz, $CDCl_3$) δ 4.3, 5.3, 6.5, 6.7, 9.9, 14.3, 20.9, 22.4, 23.4, 26.0, 29.7, 37.3, 43.4, 45.9, 56.6, 58.8, 70.3, 72.2, 72.7, 74.7, 74.9, 75.1, 76.6, 78.2, 78.5, 81.6, 84.2, 113.0, 117.2, 118.6, 121.1, 126.6, 127.6, 128.5, 128.6, 129.6, 129.9, 132.5, 132.8, 132.9, 133.4, 135.4, 136.4, 139.0, 157.1, 164.6, 165.6, 169.4, 170.0, 171.2, 201.0; HRMS (FAB/DCM/NaCl) *m/z* calcd for $C_{65}H_{87}NO_{16}Si_2H^+$ 1194.5462, found 1194.5509 (Δ = 3.9 ppm).

Macrocyclic Taxoid 1c (*E* and *Z*). To a solution of **7c** (108 mg, 0.09 mmol) in dry CH_2Cl_2 (25 mL) was added $Cl_2Ru(=CHPh)(PCy_3)_2$ (17 mg, 0.022 mmol) in dry CH_2Cl_2 (1 mL) under a nitrogen atmosphere. The reaction was stirred for 3 days at reflux to convert all of the starting materials. Solvent was removed in vacuo. Two products were separated by flash chromatography on silica gel (hexanes/EtOAc = 4/1−3/1) to afford **8c-*E*** as a crude yellow solid (42 mg, 40%) and **8c-*Z*** as a crude yellow solid (44 mg, 42%).

To a solution of **8c-*E*** (35 mg) in CH_3CN (0.7 mL) and pyridine (0.7 mL) was added HF−pyridine (70:30, 0.35 mL) at 0 °C under nitrogen, and the mixture was stirred overnight. Ethyl acetate (60 mL) was added to the reaction mixture, and the resulting solution was washed with saturated aqueous $NaHCO_3$ (10 mL × 2), aqueous $CuSO_4$ (8 mL × 3), water (10 mL × 3), and brine (5 mL). The organic layer was dried over anhydrous $MgSO_4$, and solvent was removed in vacuo. Flash chromatography of the residue on silica gel (hexanes/EtOAc = 1/2) afforded **1c-*E*** as a white solid (24 mg, 85%). In the same manner, **8c-*Z*** (48 mg) was deprotected to give **1c-*Z*** as a white solid (35 mg, 91%).

Macrocyclic taxoid 1c-*E*: white solid; mp 194−196 °C; $[\alpha]^{20}_D$ −107 (*c* 12.7, $CHCl_3$); ^{1}H NMR (400 MHz, $CDCl_3$) δ 1.08 (s, 3 H), 1.12 (s, 3 H), 1.60 (s, 3 H), 1.64 (s, 3 H), 1.78−1.86 (m, 1 H), 2.13 (s, 3 H), 2.34 (s, 1 H), 2.36 (s, 3 H), 2.44−2.56 (m, 1 H), 3.27 (s, 1 H), 3.69−3.77 (m, 3 H), 4.08−4.19 (m, 3 H), 4.30−4.33 (m, 3 H), 4.60−4.68 (m, 2 H), 4.92 (d, J = 8.4 Hz, 1 H), 5.57 (d, J = 15.6 Hz, 1 H), 5.82 (dd, J = 3.2, 9.2 Hz, 1 H), 5.86 (d, J = 7.2 Hz, 1 H), 5.94 (m, 1 H), 6.16 (s, 1 H), 6.25 (d, J = 6.0 Hz, 1 H), 6.89 (d, J = 8.4 Hz, 1 H), 7.04 (t, J = 7.6 Hz, 1 H), 7.17−7.24 (m, 3 H), 7.40 (t, J = 7.6 Hz, 3 H), 7.47 (d, J = 7.2 Hz, 2 H), 7.53 (t, J = 7.2 Hz, 1 H), 7.92 (dd, J = 7.6, 1.2 Hz, 1 H), 8.02 (d, J = 7.6 Hz, 2 H), 8.52 (d, J = 9.2 Hz, 1 H); ^{13}C NMR (100 MHz, $CDCl_3$) δ 9.4, 15.3, 20.7, 22.2, 22.5, 26.2, 29.7, 35.6, 43.2, 45.1, 54.8, 58.9, 69.1, 72.1, 72.9, 74.5, 75.3, 76.3, 77.1, 81.5, 83.5, 84.3, 112.3, 121.5, 122.7, 123.9, 127.5, 127.6, 128.1, 128.6, 129.6, 129.9, 131.7, 132.0, 132.9, 133.6, 134.4, 136.9, 138.7, 156.4, 165.2, 165.7, 170.3, 171.0, 202.9; HRMS *m/z* calcd for $C_{51}H_{55}NO_{16}H^+$ 938.3599, found 938.3590 (Δ = −0.9 ppm).

Macrocyclic taxoid 1c-*Z*: white solid; mp 166−168 °C; $[\alpha]^{20}_D$ −73 (*c* 3.7, $CHCl_3$); ^{1}H NMR (500 MHz, $CDCl_3$) δ 1.22 (s, 3 H), 1.24 (s, 3 H), 1.69 (s, 3 H), 1.84 (s, 3 H), 1.87 (m, 1 H), 2.04 (s, 3 H), 2.24 (s, 3 H), 2.40 (d, J = 4.0 Hz, 1 H), 2.50−2.51 (m, 1 H), 2.97 (d, J = 8.5 Hz, 1 H), 3.44 (s, 1 H), 3.74 (d, J = 7.5 Hz, 1 H), 3.85 (d, J = 8.0 Hz, 1 H), 4.14 (d, J = 11.0 Hz, 1 H), 4.19 (d, J = 8.0 Hz, 1 H), 4.20 (d, J = 8.5 Hz, 1 H), 4.34−4.44 (m, 3 H), 4.60 (dd, J = 12.5, 8.5 Hz, 1 H), 4.91 (d, J = 9.0 Hz, 1 H), 5.03 (dd, J = 8.5, 3.5 Hz, 1 H), 5.49 (dd, J = 5.5, 4.0 Hz, 1 H), 5.70−5.77 (m, 1 H), 5.82 (t, J = 9.0 Hz, 1 H), 5.92 (d, J = 7.5 Hz, 1 H), 6.20 (d, J = 6.5 Hz, 1 H), 6.28 (s, 1 H), 7.00 (d, J = 8.0 Hz, 1 H), 7.24−7.26 (m, 1 H), 7.34−7.44 (m, 7 H), 7.60−7.66 (m, 2 H), 8.03 (d, J = 7.5 Hz, 2 H), 8.35 (dd, J = 7.5, 1.0 Hz, 1 H), 8.49 (d, J = 6.0 Hz, 1 H); ^{13}C NMR (100.5 MHz, $CDCl_3$) δ 9.4, 14.7, 20.8, 22.2, 23.4, 26.2, 35.4, 43.4, 44.9, 58.6, 59.5, 63.3, 71.1, 71.9, 72.8, 72.9, 75.2, 75.9, 77.2, 78.0, 78.6, 78.8, 81.0, 84.3, 111.8, 122.2, 123.2, 128.1, 128.6, 128.7, 129.7, 129.9, 132.8, 133.5, 133.6, 134.6, 134.7, 135.4, 138.2, 156.3, 165.1, 165.6, 169.9, 171.1, 174.1, 202.9; HRMS *m/z* calcd for $C_{51}H_{55}NO_{16}H^+$ 938.3599, found 938.3589 (Δ = −1.0 ppm).

Macrocyclic Taxoid 1d (SB-T-2061). To a solution of **7d** (45 mg, 0.04 mmol) in CH_2Cl_2 (20 mL) was added $Cl_2Ru(=CHPh)(PCy_3)_2$ (8 mg, 0.009 mmol) in CH_2Cl_2 (10 mL). The reaction was stirred overnight, and solvent was removed by reduced pressure vacuum. The residue was passed through a short silica gel column to remove the catalyst to afford **8d** as a yellow solid (80%).

To a solution of **8d** thus obtained in CH_3CN (1.0 mL) and pyridine (1.0 mL) was added HF−pyridine (70:30, 0.5 mL), and the reaction mixture was stirred overnight. The reaction mixture was quenched with EtOAc (100 mL) and washed with saturated aqueous $NaHCO_3$ solution (10 mL), $CuSO_4$ solution (10 mL × 3), water (10 mL × 3), and brine (3 mL). The organic layer was dried over anhydrous $MgSO_4$, and solvent was removed under reduced pressure. The residue was purified by a column chromatography on silica gel using hexanes/EtOAc (2:1) as the eluent to afford **1d** as white solid (83%): mp 198−200 °C; ^{1}H NMR (300 MHz, $CDCl_3$) δ 1.19 (s, 3 H), 1.23 (s, 3 H), 1.72 (s, 3 H), 1.90 (s, 3 H), 1.91 (s, 3 H), 1.92 (s, 3 H), 2.27 (s, 3 H), 2.39 (s, 3 H), 3.23−3.28 (m, 2 H), 3.80−3.82 (m, 2 H), 3.88 (d, J = 5.1 Hz, 1 H), 3.98−4.05 (m, 2 H), 4.25 (d, J = 5.4 Hz, 1 H), 4.40−4.48 (m, 2 H), 4.54 (d, J = 3.6 Hz, 1 H), 5.02 (d, J = 5.4 Hz, 1 H), 5.19−5.31 (m, 2 H), 5.49 (d, J = 9.3 Hz, 1 H), 5.68−5.77 (dt, J = 15.0, 6.3 Hz, 1 H), 5.99 (d, J = 7.2 Hz, 1 H), 6.16 (dd, J = 7.8, 1.8 Hz, 1 H), 6.31−6.35 (m, 2 H), 7.18−7.21 (m, 1 H), 7.29−7.34 (m, 1 H), 7.38−7.55 (m, 4 H), 7.64−7.66 (m, 1 H), 8.09−8.13 (m, 2 H); ^{13}C NMR (62.9 MHz, $CDCl_3$) δ 9.4, 14.9, 18.8, 20.8, 22.4, 22.9, 26.1, 35.5, 36.1, 43.4, 45.0, 49.8, 58.8, 72.0, 72.5, 74.5, 75.2, 77.1, 80.3, 81.5, 84.3, 118.5, 126.4, 126.8, 127.6, 128.6, 129.4, 130.0, 130.5, 131.1, 131.7, 133.7, 134.5, 135.7, 137.4, 138.3, 140.8, 165.2, 168.9, 170.0, 171.1, 171.8, 202.9; HRMS calcd for $C_{49}H_{57}NO_{15}H^+$ 900.3806, found 900.3805 (Δ= 0.2 ppm).

Macrocyclic Taxoid 9b (SB-T-2054). To a solution of **7b** (43 mg, 0.036 mmol) in CH_2Cl_2 (22 mL) was added $Cl_2Ru(=CHPh)(PCy_3)_2$ (8 mg × 3, 0.027 mmol) in CH_2Cl_2 (0.08 mL). The reaction was refluxed for 5 days, and solvent was removed by reduced pressure vacuum. The residue was passed through a short column (eluent: hexanes/EtOAc = 3/1) to remove the catalyst to afford **8b** as a crude yellow solid (20 mg, 50%) with unreacted diene (**7b**, 11 mg, 25%) recovered.

To a solution of **8b** (20 mg) in CH_3CN (0.4 mL) and pyridine (0.4 mL) was added HF−pyridine (70:30, 0.2 mL), and the reaction mixture was stirred overnight. The reaction mixture was quenched with EtOAc (50 mL) and washed with saturated aqueous $NaHCO_3$ solution (10 mL × 2), $CuSO_4$ solution (10 mL × 3), water (10 mL × 3), and brine (3 mL). The organic layer was dried over anhydrous $MgSO_4$, and solvent was removed under reduced pressure. The

residue was purified by a column chromatography on silica gel using hexanes/EtOAc (1:1) as the eluent to afford **9b** as a white solid (13 mg, 80%): mp 203−205 °C; $[\alpha]^{22}_{D}$ −28 (*c* 0.92, $CHCl_3$); ^{1}H NMR (600 MHz, $CDCl_3$) δ 1.19 (s, 3 H), 1.23 (s, 3 H), 1.72 (s, 3 H), 1.73 (s, 3 H), 1.91 (m, 1 H), 1.94 (m, 1 H), 2.23 (s, 3 H), 2.24 (m, 1 H), 2.57 (m, 1 H), 2.63 (s, 3 H), 3.35 (s, 1 H), 3.49 (t, J = 9.6 Hz, 1 H), 3.82 (m, 3 H), 4.26 (d, J = 8.4 Hz, 1 H), 4.38 (m, 1 H), 4.40 (d, J = 8.4 Hz, 1 H), 4.78 (m, 1 H), 5.00 (d, J = 6.8 Hz, 1 H), 5.62 (d, J = 7.8 Hz, 1 H), 5.92 (ddd, J = 16.8, 8.4, 2.8 Hz, 1 H), 6.02 (d, J = 7.2 Hz, 1 H), 6.31 (s, 1 H), 6.36 (d, J = 7.8 Hz, 1 H), 6.52 (d, J = 16.2 Hz, 1 H), 6.90 (d, J = 8.4 Hz, 1 H), 7.22 (d, J = 7.2 Hz, 1 H), 7.34−7.63 (m, 10 H), 8.10 (d, J = 7.8 Hz, 2 H); ^{13}C NMR (75.5 MHz, $CDCl_3$) δ 9.1, 15.1, 20.8, 23.0, 23.3, 26.2, 29.7, 32.7, 35.7, 43.6, 44.9, 54.6, 58.9, 72.1, 72.7, 73.3, 75.2, 76.4, 77.2, 77.9, 79.0, 81.6, 84.3, 126.5, 126.7, 126.8, 128.3, 128.4, 128.8, 128.9, 129.0, 129.2, 129.9, 130.0, 131.1, 133.7, 134.9, 135.0, 136.6, 137.9, 138.4, 165.4, 169.4, 170.1, 171.1, 173.2, 202.9; HRMS (FAB/DCM/NaCl) *m*/*z* calcd for $C_{51}H_{55}NO_{15}H^+$ 922.3650, found 922.3643 (Δ = −0.8 ppm).

X-ray Single-Crystal Analysis of 9b (SB-T-2054). A colorless single crystal (0.2 × 0.3 × 0.5 mm^3) of **9b** grown in a NMR tube by slow diffusion of hexanes (0.5 mL) into a solution of **9b** (5 mg) in a mixture of dichloromethane (0.1 mL) and ethyl actate (0.05 mL) was selected for X-ray crystallographic analysis. Since the crystals obtained in this way were sensitive to air, the test single crystal was sealed along with some mother liquid in a capillary tube. Intensity data collection was carried out with a Bruker AXS SMART diffractometer equipped with a CCD detector using a Siemens graphite-monochromated Mo radiation tube (λ = 0.71073 Å) at room temperature. The unit cells were determined by a least-squares analysis using the SMART software package. The raw frame data were integrated into SHELX-format reflection files and corrected for Lorentz and polarization effects using SAINT. Corrections for incident and diffracted beam absorption effects were applied using SADABS. The structure was solved by direct method and refined by full-matrix least-squares method on *F*2 using the SHELXTL 97 software package. All non-hydrogen atoms were refined anisotropically. Hydrogen atoms were placed in calculated positions and added as fixed contributions. There are solvent molecules trapped in the crystals. However, we were not able to fully solved the structure due to their highly disordered behavior. Ignorance of these solvent molecules did not terribly harm the final refinement; thus, we simply treated this single crystal as a solvent free sample. The CIF file is available as Supporting Information.

In Vitro Cell Growth Inhibition Assay. Tumor cell growth inhibition was determined according to the method established by Skehan et al.[38] Human cancer cells LCC6-WT (Pgp-), MCF-7 (Pgp-), LCC6-MDR (Pgp+), NCI/ADR (Pgp+), A2780 (Pgp-), and HT-29 (Pgp-) were plated at a density of 400−2000 cells/well in 96-well plates and allowed to attach overnight. These cell lines were maintained in RPMI-1640 medium (Roswell Park Memorial Institute growth medium) supplemented with 5% fetal bovine serum and 5% Nu serum (Collaborative Biomedical Product, MA). Macrocyclic axoids were dissolved in DMSO and further diluted with RPMI-1640 medium. Triplicate wells were exposed to various treatments. After 72 h incubation, 100 μL of ice-cold 50% trichloroacetic acid (TCA) was added to each well, and the samples were incubated for 1 h at 4 °C. Plates were then washed five times with water to remove TCA and serum proteins, and 50 μL of 0.4% sulforhodamine B (SRB) was added to each well. Following a 5 min incubation, plates were rinsed five times with 0.1% acetic acid and air-dried. The dye (SRB) was then solubilized with 10 mM Tris base (pH 10.5) for 5 min on a gyratory shaker. Optical density was measured at 570 nm. The IC_{50} values were then calculated by fitting the concentration−effect curve data with the sigmoid-E_{max} model using nonlinear regression, weighted by the reciprocal of the square of the predicted effect. [39]

Tubulin Polymerization Assay. Assembly and disassembly of calf brain microtubule protein (MTP) was monitored spectrophotometrically (Beckman Coulter DU 640, Fullerton, CA) by recording changes in turbidity at 350 nm at 37 °C.[40,41] MTP was diluted to 1 mg/mL in MES buffer containing 3 M glycerol. The concentration of tubulin in MTP is 85%, and that is taken into consideration when the ratios of tubulin to drug are presented in Figure 6. Microtubule assembly was carried out with 10 μM **9b** (SB-T-2054). Paclitaxel (10 μM) and GTP (1 mM) were also used for comparison purposes. Calcium chloride (6 mM) was added to the assembly reaction after 50 min to follow the calcium-induced microtubule depolymerization.

Electron Microscopy. Aliquots (50 μL) were taken from in vitro polymerization assays at the end of the reaction and placed onto 300-mesh carbon-coated, formavar-treated copper grids. Samples were then stained with 20 μL of 2% uranyl acetate and viewed with a JEOL Model 100CX electron microscope.

Computational Methods. The structures of the C14−C3′BzN-linked macrocyclic taxoids **1a**, **1c-*E***, **1c-*Z***, and **9b** in the 1JFF were produced by directly introducing the linker into the "REDOR-Taxol" in the 1JFF complexes using the Builder module in the InsightII 2000 program (CVFF). Then, these structures were energy-minimized in 5000 steps or until the maximum derivative was <0.001 kcal/A by means of the conjugate gradients method using the CVFF force field and the distance-dependent dielectric. The backbone of the protein was fixed throughout the energy minimization. After the energy minimization, the snapshots were overlaid by superimposing the backbones of the proteins. During the energy minimizations of the macrocyclic taxoids, the C′2-OH-N(His^{227}) H-bond was very stable in all cases. Monte Carlo conformational searches on the C14−C3′BzN-linked macrocyclic taxoids were performed with energy minimization (5000 MC steps, minimization for 1000 steps with Polak-Ribiere conjugated gradients) by Macromodel program using a generalized born with surface area term (GBSA) continuum solvent description of water solvation.[42]

Acknowledgment. This work was supported by grants from the National Institutes of Health (CA103314 and GM42798 to I.O.; CA083185 and CA077263 to S.B.H.; CA 73872 to R.J.B.) and the National Science Foundation (PACI-MCA02N028 to C.S.). Generous support from Indena, SpA is also gratefully acknowledged. L.S. and I.O. also thank Ms. Rebecca Rowehl for her valuable help at the Cell Culture and Hybridoma Facility at Stony Brook.

Supporting Information Available: Refined "REDOR-Taxol" structure; Monte Carlo conformational search and analysis results for **1a**, **1c-*E***, **1c-*Z***, and **9b**; ^{1}H and ^{13}C NMR spectra of **3a−d**, **6**, **7a−d**, **1a**, **1c-*E***, **1c-*Z***, **1d**, and **9b**; single-crystal X-ray analysis data for **9b**. This material is available free of charge via the Internet at http://pubs.acs.org.

JO801713Q

(38) Skehan, P.; Storeng, R.; Scudiero, D.; Monks, A.; McMahon, J.; Vistica, D.; Warren, J. T.; Bokesch, H.; Kenney, S.; Boyd, M. R. *J. Nat. Cancer Inst.* **1990**, *82*, 1107–1112.

(39) Motulsky, H. J.; Ransnas, L. A. *FASEB J.* **1987**, *1*, 365–74.

(40) Weisenberg, R. C. *Science* **1972**, *177*, 1104–1105.

(41) Shelanski, M. L.; Gaskin, F.; Cantor, C. R. *Proc. Natl. Acad. Sci. U.S.A.* **1973**, *70*, 765–768.

(42) Still, W. C.; Tempczyk, A.; Hawley, R. C.; Hendrickson, T. *J. Am. Chem. Soc.* **1990**, *112*, 6127–9.